ESTIMATING RUNNING SAFETY FACTOR OF BALLASTLESS RAILWAY BRIDGES USING TAIL MODELLING

Reza Allahvirdizadeh*, Andreas Andersson, Raid Karoumi

KTH Royal Institute of Technology, Division of Structural Engineering & Bridges, Department of Civil and Architectural Engineering, Brinellvägen 23, 100 44 Stockholm, Sweden

* corresponding author: `rezaal@kth.se`

ABSTRACT. Excessive vertical acceleration of ballastless railway bridges subjected to vibrations induced by passing trains is one of the governing design criteria for bridges in high-speed lines. However, to the authors' knowledge, the corresponding design limit is not based on a solid theoretical or experimental background. Moreover, the traditionally applied safety factor also suffers from these concerns. Therefore, in the present study, a crude probabilistic approach is adopted to evaluate the consistency and reliability of this safety factor. For this purpose, deterministically designed bridges (using conventional methods) with short to medium spans are considered. Then, their reliability is evaluated using simulation-based techniques and extreme value theory, i.e., tail approximation. Then, the existing safety factor is calculated to evaluate the consistency of the current approaches, and possible new values are proposed based on the desired target reliabilities.

KEYWORDS: Ballastless bridges, high-speed railway bridges, running safety, safety factor, structural reliability, tail modelling.

1. INTRODUCTION

The increase in operating speed of trains in recent decades leads to excessive vibration of infrastructure, especially bridges, which raises new safety concerns. Such vibrations can affect the structural performance of bridges, jeopardize the safe passage of trains on bridges (denoted here as *running safety*), and disrupt passenger comfort.

Ensuring running safety requires preventing loss of contact between wheels and rail, the occurrence of which increases the risk of train derailment. This phenomenon can be formulated as an unloading ratio, which reads as Eq.(1) [1].

$$\frac{\Delta P}{P_{\text{st}}} = \frac{P_{\text{st}} - P_{\text{min,dyn}}}{P_{\text{st}}} \qquad (1)$$

where P_{st} is the static vertical wheel load and $P_{\text{min,dyn}}$ is the minimum dynamic vertical wheel load. Theoretically, contact loss occurs at a unloading ratio of 1, but [1] limits this to 0.6.

Considering the formulation presented, the study of the running safety problem must take into account various subsystems, namely the passing train, the rail, the track, the bridge components, the boundary conditions, and the interaction between all these subsystems. The train and the track are coupled to each other by the interactive wheel-rail force, which is transmitted to the bridge through the track. It is worth noting that there are a variety of track types in the world, which can generally be categorized into two classes: Ballasted and ballastless (also referred to as Non-Ballasted or Slab Track). For the first type, a granular material is formed between the sleepers and the bridge deck. For the latter, however, there

are different construction methods, about which the interested reader can find a detailed overview in [2], but in general they consist of two concrete layers and a bituminous mixture in between.

Clearly, the use of such complicated computational models requires a high level of expertise and involves expensive computational costs. Therefore, for practical purposes, moving load models are often used, which are computationally very efficient. In addition, it has been shown that such reduced models can lead to acceptably accurate answers when the train weight is much smaller than the bridge (which seems to be the case for passenger trains) and also in cases where the study of the dynamic behavior of trains is not sought [3]. This approach cannot model the contact loss between wheels and rail. Therefore, the design rules implicitly control the ride safety criterion by instead limiting the vertical acceleration of the bridge deck [4] or its deflection [5].

This assumes that contact loss occurs at accelerations greater than 1.0 g; however, the authors found no theoretical or experimental justification for this assumption. The relationship between this criterion and the unloading ratio (wheel-rail contact loss) was previously studied using train-track-bridge interaction (TTBI) models, where it was found that the acceleration criterion almost always dominates the design [6, 7].

In addition, an arbitrary safety factor of 2 is applied to the above threshold. Therefore, the maximum allowable vertical acceleration of ballastless railroad bridges should be limited to 5 m/s². This safety factor is borrowed from the phenomenon of ballast instability [4]; however, it should be emphasized that the consis-

tency and reliability of this safety factor is questioned even for bridges with ballast [8]. Considering this situation, a rough probabilistic approach is taken in this article to evaluate the reliability of the conventional safety factor for ballastless railroad bridges.

The rest of this article is divided into the review of the applied reliability assessment method in 2, the description of the constructed computational models in 3, the formulation of the reliability problem in 4, and the estimation of the corresponding safety factors in 5. The article concludes with a summary of the main results.

2. RELIABILITY ASSESSMENT USING TAIL MODELLING

The probability of failure (p_f) is generally estimated by calculating the presented multiple integral in Eq. (2):

$$p_f = P(g(\mathbf{X}) \leq 0) = \int_{\mathcal{D}} f_{\mathbf{X}}(\mathbf{x})d\mathbf{x} \qquad (2)$$

where $\mathbf{X} \in \mathbb{R}^m$ is the vector of basic random variables, $f_{\mathbf{X}}(\mathbf{x})$ is their joint distribution probability, and $g(\cdot)$ is the limit state function. The latter is basically a decision boundary separating the failure domain ($\mathcal{D}$) from the safe region. These regions are distinguished based on the sign of the limit state function, i.e., failure occurs when $g(\mathbf{X}) = R - S \leq 0$; where R is the capacity corresponding to the failure mode and S is the demand (e.g., load, displacement, stress, or strain). At this point, it should be mentioned that reformulating the reliability problem as a ratio between action and corresponding capacity, i.e., $g(\mathbf{X}) = S/R$ instead of subtracting them, changes the failure domain to the region where $g(\mathbf{X}) \geq 1$.

The calculation of this integral is usually not tractable in real applications. This is because the joint probability distribution of the basic random variables and the failure domain are generally not available. Therefore, a variety of methods have been developed to overcome these problems. The best known of these are crude Monte-Carlo simulation (MC) and first and second order reliability methods (FORM /SORM).

The crude MC gives the most accurate estimate of the failure probability, making it the most widely applicable approach. It can be expressed as Eq. (3):

$$p_f = \int \mathbb{I}[g(\mathbf{X}) \leq 0] f_{\mathbf{X}}(\mathbf{x})d\mathbf{x} = \mathbb{E}\big[\mathbb{I}[g(\mathbf{X}) \leq 0]\big]$$

$$\approx \frac{1}{N} \sum_{i=1}^{N} \mathbb{I}[g(\hat{X}_i) \leq 0] \quad (3)$$

where $\mathbb{I}(\cdot)$ is an indicator function equal to one if true and zero otherwise. Also, N is the number of realizations (samples) of the basic random variables. Although it is generally applicable, crude MC is not an efficient approach for the majority of reliability problems. This is because its accuracy (represented by the

coefficient of variation of the estimated probability of failure) is inversely proportional to the square root of the number of samples ($\propto N^{-1/2}$) and also to the order of the probability of failure. Considering that the failure probability in structural engineering is usually in the range of $10^{-4} - 10^{-3}$, performing MC incurs significant (and usually unaffordable) computational costs for reliability assessment tasks.

Moreover, FORM is basically an optimization-based solution that finds the smallest distance between the point with the largest likelihood on the transformed joint probability distribution in the standard Normal space and the most probable point (MPP). The latter should be on the limit state function approximated by the first Taylor expansion around the MPP.Therefore, FORM reads as Eq. (4).

$$\beta = \arg\min_{\mathbf{t}} \quad \frac{1}{2}\mathbf{t}^T\mathbf{t}$$
$$\text{s.t.} \quad G(\mathbf{t}) = 0 \qquad (4)$$

where $\beta = -\Phi^{-1}(p_f)$ is the safety index, $\mathbf{t} = T(\mathbf{X})$ is the transformed basic random variables transformed into the standard Normal space, and $G(\cdot)$ is the reformulated limit state function based on the transformed variables. It is worth noting that basic random variables can be transformed into standard Normal space, for example, using the Nataf transformation [9]. An application of FORM to evaluate the running safety of ballasted high-speed railway bridges is presented in [8]. As mentioned earlier, this method is computationally efficient but may not be accurate enough for highly nonlinear limit- state functions [10, 11].

Considering the discussed issues regarding the efficiency and accuracy of classical reliability assessment techniques, they were later improved by the introduction of more advanced methods. These include Important Sampling (IS) [10, 12], Subset Simulation (SS) [13], Surrogate-based approaches [14, 15], and Tail Estimation (approximation). The explanation of these methods is beyond the scope of this article; therefore, the interested reader is referred to the references provided. Therefore, only the latter approach used in this study is explained here.

The failure event is usually a rare event among all possible scenarios of a designed system; therefore, the failure probability is located at the tails of the cumulative distribution function (CDF) of the limit-state function. Thus, the basic idea of tail modeling is to approximate the tail of the true distribution by another distribution with an equivalent tail by running a limited number of simulations. The tail equivalence property reads as [16]:

$$\lim_{g(x) \to \infty} \frac{1 - T[g(X)]}{1 - F[g(X)]} = 1 \qquad (5)$$

where $F[g(\mathbf{x})]$ and $T[g(\mathbf{x})]$ are CDF of the limit state function and that of the tail model, respectively. This equivalence holds for the tails of the true CDF (upper

or lower ones); therefore, a threshold (denoted here as u) should be chosen to fit the tail model for values larger (or smaller) than this. This results in the fitted tail being formulated based on a transformed variable called the exceedance ($z = x - u$). The concept of tail approximation, threshold, and exceedance is shown schematically in Figure 1. It should be noted here that the limit-state function in Figure 1 has been reformulated to show the region of failure at the upper end for illustrative purposes.
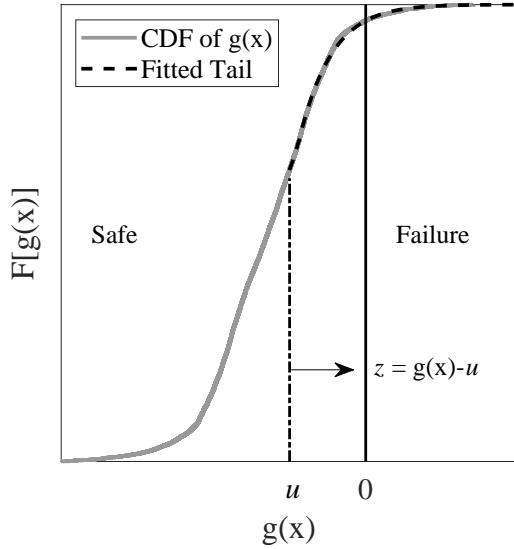
FIGURE 1. Concept of tail modelling.

The most widely used tail model is the generalized Pareto distribution (GPD), given as Eq.(6). In addition, the sigmoid (Eq.(7)) and exponential functions have been used for reliability assessment of high-speed railway bridges in [17], where it was concluded that the sigmoid function can lead to a more accurate estimate of the probability of failure.

$$T_Z(z) = \begin{cases} 1 - \left\langle 1 + kz/\psi \right\rangle_+^{-1/k} & k \neq 0 \\ 1 - \exp(-z/\psi) & k = 0 \end{cases} \quad (6)$$

$$T_Z(z) = c_1 + \frac{c_2}{\left[1 + \exp\left(z/c_3\right)\right]^{c_4}} \quad (7)$$

where k is the shape parameter of GPD, ψ its scale parameter, $c_i, \ i = 1, ..., 4$ are constants of the sigmoid function, and $\langle A \rangle_+ = \max(0, A)$. These parameters can be calculated using either the maximum likelihood method (MLE) or the least squares method (regression).

In [18], it was shown that using a single-tail model does not guarantee that the failure probability is always estimated accurately. Therefore, they proposed to calculate the probability of failure based on a linear regression on the safety index of the top 10% of the data (Beta- LT), a quadratic polynomial fit to the top 50% of the safety index data (Beta- QH), and

a quadratic fit to the logarithmic transformation of the safety index (LnBeta- QT) [18]. Then they proposed to use the median value of the estimated failure probability from the discussed approaches, showing for benchmark problems that it is almost always at least the second best estimate. Therefore, the same approach is followed in this study, using the sigmoid function as the tail model as well.

In addition to the assigned parameters of the tail model, its performance also depends on the threshold considered. In [19], it was proposed to consider $1.5\sqrt{N}$ (where N is the total number of data) to fit the tail model (hereafter referred to as Hasofer's method). Similarly, [20] suggests using $0.02N$ and $0.1N$ for cases of $50 < N < 500$ and $500 < N < 1000$, respectively (hereafter referred to as Boos' method). Furthermore, in [21], they discussed that thresholds close to the central data cause the fitted tail to suffer from high bias, while very large thresholds can lead to tail approximations with high variance (trade-off between bias and variance). In this context, they proposed to select the optimal threshold by calculating the mean square error (MSE) of the estimated safety index (β) at all thresholds considered. The MSE can be calculated as the sum of the squared bias and the variance of the estimated safety index at a given threshold (see Eq. (8)). Given the definition of bias (see Eq.(9)) and variance (see Eq.(10)), the expected value of the estimated safety index is needed. Therefore, they proposed to find the expected value of the safety index using the bootstrap method. An illustrative example of the latter approach is shown in Figure 2, where the horizontal axis represents the threshold value as the quantile of all data. It is worth noting that for illustration purposes, the well-known Ishigami function is used in the form of Eq. (11) to represent the limit state function [22]. Threshold selection using this approach is more robust than other methods, although it increases the computational cost. Since this additional computational cost is only at the level of post-processing existing data, it would be affordable.

$$\text{MSE}(\beta|u) = \text{Bias}^2(\beta|u) + \text{Var}(\beta|u) \quad (8)$$

$$\text{Bias}(\beta|u) = \mathbb{E}[\hat{\beta}(u)] - \beta \quad (9)$$

$$\text{Var}(\beta|u) = \mathbb{E}\big[(\hat{\beta}(u) - \mathbb{E}[\hat{\beta}(u)])^2\big] \quad (10)$$

$$f(\mathbf{x}) = 16.5 - \left[\sin(x_1) + 7\sin^2(x_2) + 0.1x_3^4 \sin(x_1)\right]$$
$$x_i \sim \mathcal{U}(-\pi, \pi) \quad i = 1, 2, 3 \quad (11)$$
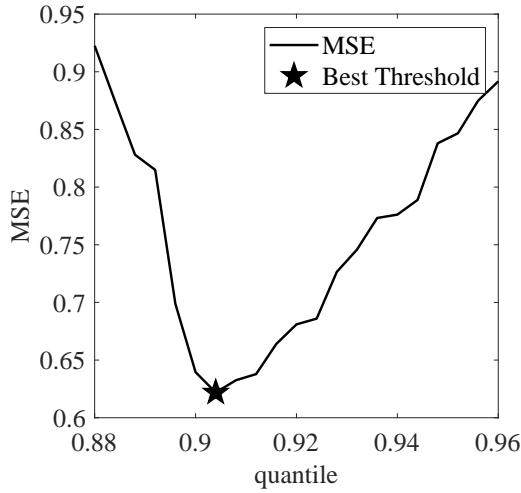
Figure 2. Threshold selection using MSE estimator.

3. Computational Model

As mentioned earlier, this study is concerned with the running safety of ballastless high-speed railway bridges. This problem consists of four subsystems, namely the passing train, the rail, the slab track and the bridge, and their interactions. The used 2D computational model of the simply supported bridges is shown in Figure 3.

The rail, slab track and bridge are modeled as Euler-Bernoulli beams. In addition, the rail pads between the rail and the slab track are modeled using lumped springs and dashpots, while the sub grades are accounted for by distributed springs and dashpots. The structure of the train (i.e., the corresponding degrees of freedom) is neglected, resulting in the train being modeled as a series of moving loads. The trains under consideration share a bogie between two adjacent coaches (known as articulated trains) and it is assumed that the axle loads are identical for each realization. Since the loads move along the rail, the components of the load vector that do not relate to the rail are zero.

Therefore, the equation of motion can be expressed as Eq. (12) using partitioned matrices. The interested reader can find detailed information about the computational model in [6, 23].

$$
\begin{bmatrix} \mathbf{M}_r & \mathbf{0} & \mathbf{0} \\ \mathbf{0} & \mathbf{M}_s & \mathbf{0} \\ \mathbf{0} & \mathbf{0} & \mathbf{M}_b \end{bmatrix} \begin{Bmatrix} \ddot{\mathbf{Y}}_r \\ \ddot{\mathbf{Y}}_s \\ \ddot{\mathbf{Y}}_b \end{Bmatrix} + \begin{bmatrix} \mathbf{C}_r & \mathbf{C}_{rs} & \mathbf{0} \\ \mathbf{C}_{sr} & \mathbf{C}_s & \mathbf{C}_{sb} \\ \mathbf{0} & \mathbf{C}_{bs} & \mathbf{C}_b \end{bmatrix} \begin{Bmatrix} \dot{\mathbf{Y}}_r \\ \dot{\mathbf{Y}}_s \\ \dot{\mathbf{Y}}_b \end{Bmatrix}
$$

$$
+ \begin{bmatrix} \mathbf{K}_r & \mathbf{K}_{rs} & \mathbf{0} \\ \mathbf{K}_{sr} & \mathbf{K}_s & \mathbf{K}_{sb} \\ \mathbf{0} & \mathbf{K}_{bs} & \mathbf{K}_b \end{bmatrix} \begin{Bmatrix} \mathbf{Y}_r \\ \mathbf{Y}_s \\ \mathbf{Y}_b \end{Bmatrix} = \begin{Bmatrix} \mathbf{F}_r \\ \mathbf{0} \\ \mathbf{0} \end{Bmatrix} \quad (12)
$$

where $\mathbf{M}$, $\mathbf{C}$, and $\mathbf{K}$ represent the mass, damping, and stiffness matrices of each subsystem, respectively. The indices r, s, and b represent rail, slab track, and bridge, respectively. Each subsystem is represented by diagonal terms and the off-diagonal partitioned matrices couple the subsystems (rail to slab and slab to bridge). The rail to slab coupling matrices include the

lumped spring and the dashpots of the railpads. Similarly, the rail to bridge coupling matrices include the distributed spring and the dashpots of the subgrade. In addition, $\mathbf{Y}$ is the vector of subsystem displacements and $\mathbf{F}_r$ is the force vector. Note that the force vector is time dependent and must be reconstructed at each step based on the position of the train.

Next, the equilibrium equations of motion are solved using the Hilber-Hughes-Taylor (HHT) direct time integration method. Then, the calculated responses are filtered using a low-pass filter whose cut-off frequency corresponds to the minimum of the third vibration frequency of the bridge or 30 Hz [24].

The constructed computational model cannot capture the effect of unevenness in the rail geometry (known as rail irregularities) on the responses of the bridge. Rail irregularities are random in nature and can be modeled by a stationary Gaussian process to generate different rail profiles [25]. Then they are treated as an additional force term using the wheel-rail contact stiffness [23]. In [26], it was shown that rail irregularities can significantly amplify the maximum vertical accelerations of the bridge. Therefore, they proposed random amplification factors as an alternative method for modeling rail irregularities. A similar approach is taken by conventional codes, but they consider it as a deterministic variable. This codified amplification factor is considered here; it reads as Eq.(13) [24] for the rails with good quality.

$$
RIA =
$$
$$
1 + \frac{\alpha}{200}\left[56e^{-(L/10)^2} + 50(\frac{Lf_1}{80} - 1)e^{-(L/20)^2}\right] \quad (13)
$$

where $\alpha = \min\left(v/22, 1\right)$, v is the train speed, L is the length of the bridge span, and f_1 is the fundamental frequency of the bridge. It should be noted that the use of RIA does not necessarily lead to conservative response predictions [26]; however, this possible drawback is neglected in this study.

Since the main objective of the article is to evaluate the consistency of the conventional safety factor, the speed of passing trains is limited to the allowable operating range, which is assumed to be 240 km/h here. This is achieved by increasing the operating speed of high-speed trains on the Swedish network by 20%, which is about 200 km/h [27]. Moreover, only the maximum response of the bridge is needed to estimate the corresponding failure probability. Therefore, the maximum vertical acceleration of the deck is calculated only for critical speeds (denoted here as v_{cr}). The critical speed corresponds to the situation where the excitation frequency of the passing train coincides with the frequency of the bridge (resonance phenomenon); this is obtained from Eq.(14) [28]. It should be noted that the maximum speed is taken into account for the cases where the critical speed was greater than the allowable speed.

FIGURE 3. 2D computational model of the ballastless railway bridge.

$$v_{cr} = \frac{D f_j}{i} \qquad j = 1, 2, 3, \ldots$$
$$i = 1, 2, 3, \ldots, 1/2, 1/3, 1/4, \ldots \quad (14)$$

where, D is the characteristic length of the coach and f_j is the jth frequency of the bridge.

4. RELIABILITY PROBLEM

As mentioned earlier, the running safety is implicitly controlled by limiting the vertical acceleration of the bridge deck. Therefore, the limit state function is formulated as Eq. (15), where failure occurs for $g(\mathbf{X}) \geq 1$.

$$g(\mathbf{X}) = \frac{a_{\max}(\mathbf{X})(1 + \chi_M)}{a_{\lim}} \quad (15)$$

where $a_{\max}(\mathbf{X})$ is the maximum vertical acceleration of the bridge deck for $\mathbf{X}$ realization of the basic random variables, $a_{\lim}$ is the maximum allowable vertical acceleration of the bridge deck (here considered as 10 m/s^2), and χ_M is the model uncertainty.

The basic random variables considered are listed in Table 1, with those related to the bridge and train properties taken from [29–31]. Note that the target bridges have spans of 10 m, 20 m, and 30 m, and the values given in Table 1 are in the same order. The mean values of the cross-sectional moment of inertia and mass per length correspond to the minimum allowable values satisfying conventional deterministic design methods [29]. The nominal values of the other parameters are taken from [6, 7]; the assigned distribution function and standard deviations are based on recommendations from [32] and the authors' engineering judgment.

5. SAFETY FACTOR ESTIMATION

The objective of the article is achieved by first calculating the maximum vertical acceleration of the bridges for passing trains with critical speeds. In this context, the sensitivity of the estimated safety indices is first evaluated with respect to the number of samples considered (see Figure. 4). It should be emphasized here that the analyzes for this task were performed only for trains with a speed of 240 km/h. As can be seen, the method almost converges when the number of samples exceeds 10,000; however, 20,000 samples are considered in this study.

FIGURE 4. Sensitivity to the number of samples.

Then, the statistical parameters (i.e., mean and standard deviation) of demand are estimated by calculating the 99% quantile of these parameters using the bootstrap method. Then, the system's probability of failure is calculated using the tail approximation method. This is done by calculating the median of the probabilities of failure resulting from the methods discussed. These methods include fitting GPD by the maximum likelihood method using the Hasofer, Boos, and minimum MSE thresholds, fitting the sigmoid function by the regression method using the minimum MSE threshold, Beta- LT, Beta- QH, and LnBeta-QT. Some examples of such approaches obtained for the 30 m span bridges are shown in Figure 5.

Then, Eq. (16) is used to estimate the existing safety factor of the conventionally designed bridges. This equation is developed in [10] for linear limit-state

Variable	Dist.*	Mean/Min./Scale	Std/Max./Shape	Truncation
		Bridge		
I_b (m^4) - Moment of inertia	$\mathcal{N}$	[0.4, 1.5, 5.9]	$0.01\mu_{I_b}$	-
m_b (kg/m) - Mass per length	$\mathcal{N}$	[19000, 29000, 39000]	$0.03\mu_{m_b}$	-
ξ_b (%)† - Damping ratio	$\mathcal{LN}$	$\max(1.5 + 0.07(20 - L), 1.5)$	0.3	-
E_b (GPa) - Modulus of elasticity	$\mathcal{N}$	29.7	3.56	-
		Train		
D (m) - Coach length	$\mathcal{U}$	17	28	-
d_{BA} (m) - Axle distance	$\mathcal{U}$	2	3.5	-
p (kN) - Axle load	$\mathcal{W}$	194.93	9.14	≤ 120
		Rail		
I_r (m^4) - Moment of inertia	$\mathcal{N}$	2×61.1e-6	$0.01\mu_{I_r}$	-
m_r (kg/m) - Mass per length	$\mathcal{N}$	7850×15.38e-3	$0.03\mu_{m_r}$	-
E_r (GPa) - Modulus of elasticity	$\mathcal{N}$	205	5	-
		Slab Track		
t_s (m) - Thickness	$\mathcal{N}$	0.3	0.01	-
b_s (m) - Width	$\mathcal{N}$	2.5	0.005	-
ρ_s (kg/m^3) - Mass density	$\mathcal{N}$	2500	100	-
ξ_s (%)† - Material damping	$\mathcal{LN}$	2	0.3	-
		Rail pad		
k_{rp} (MN/m) - Stiffness	$\mathcal{N}$	2×22.5	$0.01\mu_{k_{rp}}$	-
ξ_{rp} (%)† - Damping ratio	$\mathcal{LN}$	10	0.3	-
		Slab Subgrade		
k_{sg} (MN/m^3) - Stiffness	$\mathcal{N}$	100	$0.2\mu_{k_{rp}}$	-
ξ_{sg} (%)† - Damping ratio	$\mathcal{LN}$	2	0.3	-
		Model Uncertainty		
χ_M (-) - Model uncertainty	$\mathcal{N}$	0	0.086	-

* $\mathcal{N}$, $\mathcal{LN}$, $\mathcal{U}$ and $\mathcal{W}$ indicate normal, lognormal, uniform and Weibull distributions, respectively.

† Parameters are in physical space.

TABLE 1. Considered basic random variables.

functions using the separation function to linearize its standard deviation.

$$\gamma = \frac{1 + \theta\beta_C \text{CoV}_a}{1 + k_a \text{CoV}_a} \quad (16)$$

where $\theta = 0.75 \pm 0.06$ for $1/3 < \sigma/\mu < 3$ is the separation constant linearizing the standard deviation of the linear limit state function, i.e. $\sigma_Z = (\sigma_R^2 + \sigma_S^2)^{1/2}$ changes to $\sigma_Z \approx \theta(\sigma_R + \sigma_S)$ for limit state functions in the form of $G(\mathbf{X}) = R - S$. Also, β_C is the safety index corresponding to the limit state under consideration, CoV_a is the coefficient of variation of the demand (here the vertical acceleration of the bridge deck), and k_a is the standardized characteristic value (95% quantile - denoted here as a_k) of the demand, which reads as $k_a = (a_k - \mu_a)/\sigma_a$.

Next, the new safety factor is calculated using the same data, replacing the existing safety index with a target safety index, which is $\beta_t = 3.719$ (i.e., $p_{f,t} = 10^{-4}$). The calculated values are given in Table 2; where γ_{exist} and γ_{new} indicate an approximation of the safety factor based on conventional design

methodology and the potential values to be adopted in the future, respectively. It should be emphasized here that minimum allowable mass values have been assigned to the bridges considered; therefore, the values presented represent an approximate lower bound of the possible safety indices.

As can be seen, the conventional design method does not result in a consistent safety factor; although an identical factor was used for the design of all bridges. This conclusion underscores the point that safety factors in the future should probably be a function of span length, rather than being constant.

In addition, bridges with shorter spans are more susceptible to higher accelerations, resulting in a lower safety factor compared to longer bridges. Considering the safety factor obtained for bridges with a span of 20 m, it is even possible that some scenarios are neoconservative. On the contrary, criteria other than running safety may dominate the design of bridges with larger spans, e.g., displacement-related criteria such as passenger comfort [30]. Therefore, a very large safety factor is estimated as a consequence of

(A) . GPD-MLE-Boos threshold

(B) . Sigmoid-regression-minimum MSE threshold

(C) . Beta-LT

(D) . LnBeta-QT
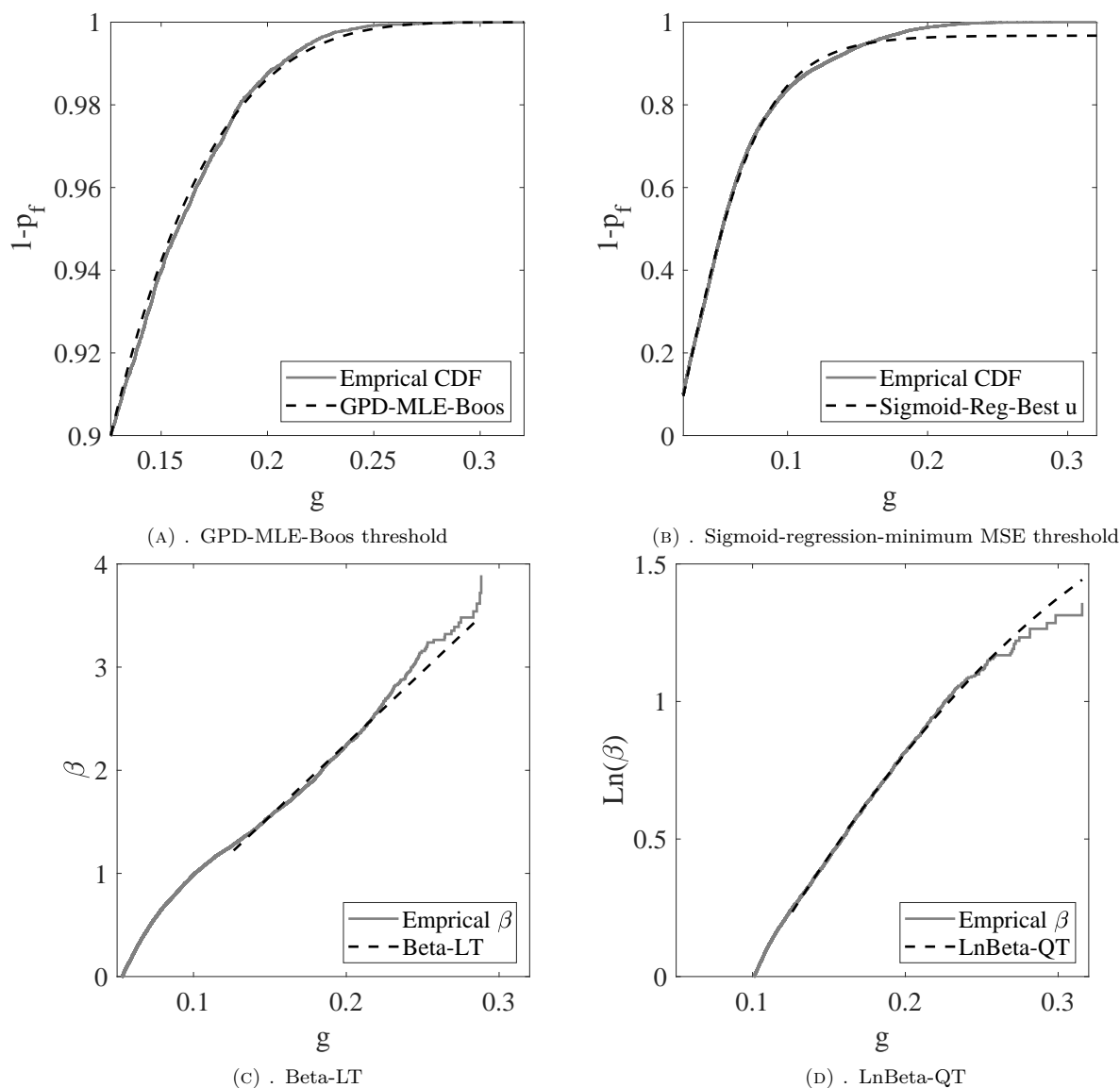
FIGURE 5. Example of fitted tail models for bridges with span length of 30 m.

L (m)	γ_{exist}	γ_{new}
10	2.91	1.18
20	1.29	1.37
30	6.46	1.17

TABLE 2. Existing and proposed safety factor for running safety of high-speed ballastless railway bridges.

a very small probability of failure. Considering this, the reliability of the estimated existing safety factor for bridges with a span of 30 m is questionable.

On the other hand, the proposed new values for the safety factor appear to be more consistent with a conservative value of about 1.4. However, as mentioned above, the use of a constant safety factor for all bridges with different spans needs to be revised.

6. CONCLUSIONS

In this study, the reliability of the conventional safety factor for the running safety of ballastless high-speed railway bridges was investigated. It was found that despite the use of a constant safety factor for bridges with different spans, the resulting designs may not have consistent safety factors. Therefore, it seems necessary to revise the current safety factor by proposing a set of new factors that depend on the span length of the bridge. In this regard, rough proposals based on an arbitrary target safety level were recommended, showing the potential of using smaller values in future design regulations.

ACKNOWLEDGEMENTS

References

[1] CEN.EN 14363. *Railway applications - testing and simulation for the acceptance of running characteristics of railway vehicles - running behaviour and stationary tests.* European Committee for Standardization, 2016.

[2] R. Bastin. Development of german non-ballasted track forms. *Proceedings of the Institution of Civil Engineers - Transport* **159**(TR1):25–39, 2006.

[3] W. Zhai, Z. Han, Z. Chen, et al. Train–track–bridge dynamic interaction: a state-of-the-art review. *Vehicle System Dynamics* **57**(7):984–1027, 2019.

[4] CEN.EN 1990/A1. *Basis of Structural Design annexe A2.* European Committee for Standardization, 2005.

[5] RTRI. *Design standards for railway structures and commentary (displacement limits).* Railway technical research institute, railway bureau of the ministry of land, infrastructure and transport government of Japan, 2007.

[6] T. Arvidsson, A. Andersson, R. Karoumi. Train running safety on non-ballasted bridges. *International journal of rail transportation* **7**(1):1–22, 2019. https://doi.org/10.1080/23248378.2018.1503975.

[7] J. Rocha. *Probabilistic methodologies for the safety assessment of short span railway bridges for high-speed traffic.* Ph.D. thesis, University of Porto, 2015.

[8] R. Allahvirdizadeh, A. Andersson, R. Karoumi. Reliability assessment of the dynamic behavior of high-speed railway bridges using first order reliability method. In *Eurodyn 2020, 11th International Conference on Structural Dynamics, Athens, 23-26 November, 2020.*, vol. 2, pp. 3438–3450. 2020. https://doi.org/10.47964/1120.9282.18654.

[9] P.-L. Liu, A. Der Kiureghian. Multivariate distribution models with prescribed marginals and covariances. *Probabilistic engineering mechanics* **1**(2):105–112, 1986.

[10] R. E. Melchers, A. T. Beck. *Structural reliability analysis and prediction.* John wiley & sons, 2018.

[11] J. D. Sørensen. *Notes in structural reliability theory and risk analysis.* Department of Civil Engineering,Aalborg University, 2011.

[12] R. Melchers. Importance sampling in structural systems. *Structural safety* **6**(1):3–10, 1989.

[13] S.-K. Au, J. L. Beck. Estimation of small failure probabilities in high dimensions by subset simulation. *Probabilistic engineering mechanics* **16**(4):263–277, 2001.

[14] B. Sudret. Meta-models for structural reliability and uncertainty quantification. *arXiv preprint arXiv:12032062* 2012.

[15] R. Allahvirdizadeh. *Reliability-Based Assessment and Optimization of High-Speed Railway Bridges.* Licentiate Thesis, KTH Royal Institute of Technology, 2021.

[16] M. A. Maes, K. Breitung. Reliability-based tail estimation. In *Probabilistic Structural Mechanics: Advances in Structural Reliability Methods*, pp. 335–346. Springer, 1994.

[17] J. Rocha, A. Henriques, R. Calçada. Safety assessment of a short span railway bridge for high-speed traffic using simulation techniques. *Engineering structures* **40**:141–154, 2012. https://doi.org/10.1016/j.engstruct.2012.02.024.

[18] P. Ramu, N. H. Kim, R. T. Haftka. Multiple tail median approach for high reliability estimation. *Structural Safety* **32**(2):124–137, 2010. https://doi.org/10.1016/j.strusafe.2009.09.002.

[19] A. Hasofer. Non-parametric estimation of failure probabilities. In F. Casciati, B. Roberts (eds.), *Mathematical models for structural reliability analysis*, chap. 4, pp. 195–226. CRC Press, 1996.

[20] D. D. Boos. Using extreme value theory to estimate large percentiles. *Technometrics* **26**(1):33–39, 1984.

[21] J. Caers, M. A. Maes. Identifying tails, bounds and end-points of random variables. *Structural Safety* **20**(1):1–23, 1998. https://doi.org/10.1016/S0167-4730(97)00036-2.

[22] T. Ishigami, T. Homma. An importance quantification technique in uncertainty analysis for computer models. In *: First International Symposium on Uncertainty Modeling and Analysis*, pp. 398–403. IEEE, 1990.

[23] P. Lou. Finite element analysis for train–track–bridge interaction system. *Archive of Applied Mechanics* **77**(10):707–728, 2007. https://doi.org/10.1007/s00419-007-0122-4.

[24] CEN. *EN 1991-2, Eurocode 1: Actions on structures - part 2: Traffic loads on bridges.* European Committee for Standardization, 2003.

[25] L. Frỳba. *Dynamics of railway bridges.* Thomas Telford Publishing, 1996.

[26] P. Salcher, C. Adam, A. Kuisle. A stochastic view on the effect of random rail irregularities on railway bridge vibrations. *Structure and Infrastructure Engineering* **15**(12):1649–1664, 2019.

[27] ERRI D 214/RP 9. Rail bridges for speeds > 200 km/h. *European Rail Research Institute* 1999.

[28] L. Frỳba. A rough assessment of railway bridges for high speed trains. *Engineering Structures* **23**(5):548–556, 2001. https://doi.org/10.1016/S0141-0296(00)00057-2.

[29] A. Andersson, R. Allahvirdizadeh, A. Zangeneh, et al. High-speed low cost bridges: background report for In2Track2, 2021.

[30] R. Allahvirdizadeh, R. Karoumi, A. Andersson. Surrogate-assisted versus subset simulation-based stochastic comparison between running safety and passenger comfort design criteria of high-speed railway bridges. In *31st European Safety and Reliability Conference (ESREL 2021).* 2021. https://doi.org/10.3850/978-981-18-2016-8_577-cd.

[31] R. Allahvirdizadeh, A. Andersson, R. Karoumi. Minimum design requirements of high-speed railway bridges using reliability-based optimization. *Unpublished Manuscript* 2021.

[32] JCSS. *JCSS Probabilistic Model Code.* Joint Committee on Structural Safety (JCSS), 2001.